Mechanism and Kinetics of Ammonium Sulfate Roasting of Boron-Bearing Iron Tailings for Enhanced Metal Extraction

Authors:

Xiaoshu Lv, Fuhui Cui, Zhiqiang Ning, Michael L. Free, Yuchun Zhai

Date Submitted: 2019-12-13

Keywords: kinetics, reaction mechanism, ammonium sulfate roasting process, iron tailings

Abstract:

The large amount of boron-bearing iron tailings in China is a resource for metals that needs to be more completely and efficiently utilized. In this evaluation, the ammonium sulfate roasting process was used to make a controllable phase transformation to facilitate the subsequent extraction of valuable metals from boron-bearing iron tailings. The effects of roasting temperature, roasting time, the molar ratio of ammonium sulfate to tailings, and the particle size on the extraction of elements were investigated. The orthogonal experimental design of experiments was used to determine the optimal processing conditions. XRD (X-Ray Diffractomer), scanning electron microscope (SEM), and simultaneous DSC?TG analyzer were used to assist in elucidating the mechanism of ammonium sulfate roasting. The experimental results showed that nearly all Fe, Al, and Mg were extracted under the following conditions: (1) the molar ratio of ammonium sulfate to iron tailings was 3:1; (2) the roasting temperature was 450 °C; (3) the roasting time was 120 min.; and, (4) the particle size was less than 80 ?m. The kinetics analysis indicated that the sulfation of metals was controlled by internal diffusion, with the apparent activation energies of 17.10 kJ·mol?1, 17.85 kJ·mol?1, 19.79 kJ·mol?1, and 29.71 kJ·mol?1 for Fe, Al, Mg, and B, respectively.

Record Type: Published Article

Submitted To: LAPSE (Living Archive for Process Systems Engineering)

Citation (overall record, always the latest version): LAPSE:2019.1592
Citation (this specific file, latest version): LAPSE:2019.1592-1
Citation (this specific file, this version): LAPSE:2019.1592-1v1

DOI of Published Version: https://doi.org/10.3390/pr7110812

processes

MDPI

Article

Mechanism and Kinetics of Ammonium Sulfate Roasting of Boron-Bearing Iron Tailings for Enhanced Metal Extraction

Xiaoshu Lv [1,2], Fuhui Cui [3,*], Zhiqiang Ning [1], Michael L. Free [4] and Yuchun Zhai [1,5]

1 School of Metallurgy, Northeastern University, Shenyang 110819, China; lvsiaoshu@163.com (X.L.); hainuo@tom.com (Z.N.); zhaiyc@smm.neu.edu.cn (Y.Z.)
2 School of Biomedical and Chemical Engineering, Liaoning Institute of Science and Technology, Benxi 117004, China
3 School of Metallurgy and Environment, Central South University, Changsha 410083, China
4 Department of metallurgical engineering, University of Utah, Salt Lake City, UT 84112, USA; michael.free@utah.edu
5 College of Resources and Materials, Northeastern University at Qinhuangdao, Qinhuangdao 066004, China
* Correspondence: fuhuicui@csu.edu.cn or cfhty0501@126.com

Received: 4 October 2019; Accepted: 24 October 2019; Published: 4 November 2019

Abstract: The large amount of boron-bearing iron tailings in China is a resource for metals that needs to be more completely and efficiently utilized. In this evaluation, the ammonium sulfate roasting process was used to make a controllable phase transformation to facilitate the subsequent extraction of valuable metals from boron-bearing iron tailings. The effects of roasting temperature, roasting time, the molar ratio of ammonium sulfate to tailings, and the particle size on the extraction of elements were investigated. The orthogonal experimental design of experiments was used to determine the optimal processing conditions. XRD (X-Ray Diffractomer), scanning electron microscope (SEM), and simultaneous DSC–TG analyzer were used to assist in elucidating the mechanism of ammonium sulfate roasting. The experimental results showed that nearly all Fe, Al, and Mg were extracted under the following conditions: (1) the molar ratio of ammonium sulfate to iron tailings was 3:1; (2) the roasting temperature was 450 °C; (3) the roasting time was 120 min.; and, (4) the particle size was less than 80 μm. The kinetics analysis indicated that the sulfation of metals was controlled by internal diffusion, with the apparent activation energies of 17.10 kJ·mol^{-1}, 17.85 kJ·mol^{-1}, 19.79 kJ·mol^{-1}, and 29.71 kJ·mol^{-1} for Fe, Al, Mg, and B, respectively.

Keywords: iron tailings; ammonium sulfate roasting process; reaction mechanism; kinetics

1. Introduction

Boron resources are abundant, but they are unevenly distributed around the world [1]. For example, Turkey, the United States, Russia, and China were the countries with the largest proved boron reserves, and collectively these countries account for about 90% of the world's total Boron reserves. China's boron reserves are the fourth largest in the world [2–4].

There are large amounts of reserves of boron resources in China, which account for 18% of the world's boron resources [4–6]. The known boron reserves are mainly distributed in northeast Liaoning, Jilin, Qinghai, and Tibet [6]. Among them, 56% of the national boron reserves are in the Liaoning province. Although the boron reserves in our country are extensive, the boron grade of the ore is very low, and the ore is mineralogically complex with a significant occurrence of economically significant metals. The complex nature of the ore requires extensive mineral processing to effectively recover the boron and the desirable metals [7,8].

There are two types of boron mineral resources in Liaoning, namely, ascharite and paigeite, which are collectively known as ludwigite. Ascharite accounts for 20% of the total reserves and it has higher boron content. After years of resource utilization, the reserve of ascharite has been depleted, and the major remaining mineral is paigeite. After magnetic separation, boron concentrates and boron-bearing iron tailings are obtained [9–11].

The boron-bearing iron tailings often contain magnesium, iron, silicon, boron, and aluminum. Currently, the boron-bearing iron tailings are processed by hydrometallurgical and pyrometallurgical methods [12]. The common hydrometallurgical methods include sulfuric acid leaching, soda leaching, ammonium sulfate leaching, and alkaline medium leaching [13–19]. The sulfuric acid leaching makes the majority of magnesium, iron, boron, and aluminum dissolve into water, and then followed by a chemical separation process. Soda and ammonium sulfate leaching have a selectivity on boron leaching, but the recovery of boron is low, and the generated slag is difficult to utilize. Alkaline leaching uses the alkali medium to dissolve boron in the style of sodium borate, the leaching efficiency of this method is high, but the serious corrosion of alkali on equipment and the huge but unrecoverable consumption of alkali restricts its developing. These methods generate waste slag and metal-bearing waste solutions, which is harmful to the environment. For the pyrometallurgical method [7,20–25], ferro-boron alloys are prepared by electric furnace smelting from boron concentrates. Smelting in a blast furnace produces ferro-boron alloys and boron-rich slags. However, these processes only recover boron from virgin ore resources. The challenges with these methods include a large amount of waste slag that is generated in the smelting process and the loss of iron and aluminum to the tailings [26].

Herein, we proposed a new process to more fully utilize boron-bearing slag. Ammonium sulfate roasting was used to make a controllable phase transformation for iron, aluminum, and boron. In the following leaching process, the silicon components in the tailings are not soluble in water. The separation of iron, magnesium, and aluminum are precipitated at different pH levels [27]. Boron is recycled based on the solubility differences between boric acid and ammonium sulfate [28,29]. The kinetics and reaction mechanisms of the roasting process were also studied, and these mechanisms have theoretical significance and reference value in the development and utilization of boron-bearing iron tailings.

2. Experimental Procedures and Materials

2.1. Materials

The boron-bearing iron tailings in this roasting evaluation were taken from Dandong, Liaoning province, China. The chemical composition of the tailings was analyzed by X-Ray Fluorescence (XRF, Bruker, S6 JAGUAR, German), and Table 1 shows the results. As seen in Table 1, the contents of boron and magnesium are high in the tailings. Ammonium sulfate that was used in this work was of analytical grade. The ammonium sulfate used in this study was obtained from Sinopharm Chemical Regent Co., Ltd. (purity > 99.0%, AR). The other regent used in the titration method was sourced from Sinopharm Chemical Regent Co., Ltd. (purity > 99.0%, AR).

Table 1. Chemical composition of the boron-bearing tailings (mass fraction, %).

MgO	CO_2	SiO_2	Fe_2O_3	B_2O_3	Al_2O_3	CaO	Na_2O	else
36.40	5.38	32.30	9.89	8.92	2.56	1.77	0.11	2.67

Figure 1 shows the X-ray diffraction patterns of the boron-bearing tailings. As presented in Figure 1, the main phases in the tailings were lizardite ($Mg_3Si_2O_5(OH)_4$), magnesium borate ($Mg_2(B_2O_5)(H_2O)$), hematite (Fe_2O_3), and cordierite ($Mg_2Si_5Al_4O_{18}$).

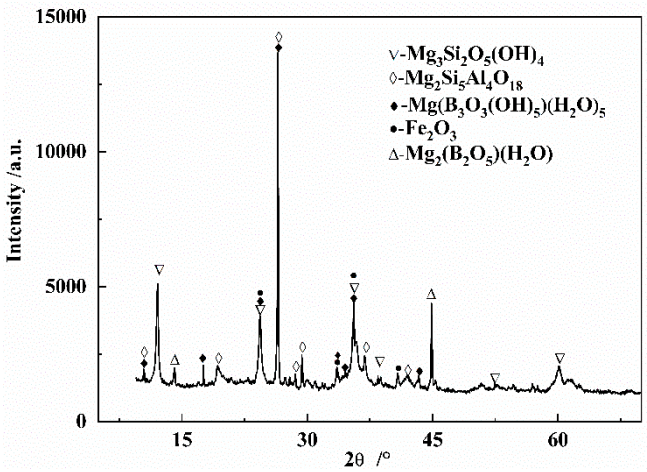

Figure 1. XRD patterns of the boron-bearing iron tailings.

Figure 2a,b show the scanning electron microscope (SEM) images of the boron-bearing iron tailings. It can be seen that the ore particles have rough surfaces, loose structures, and irregular shapes.

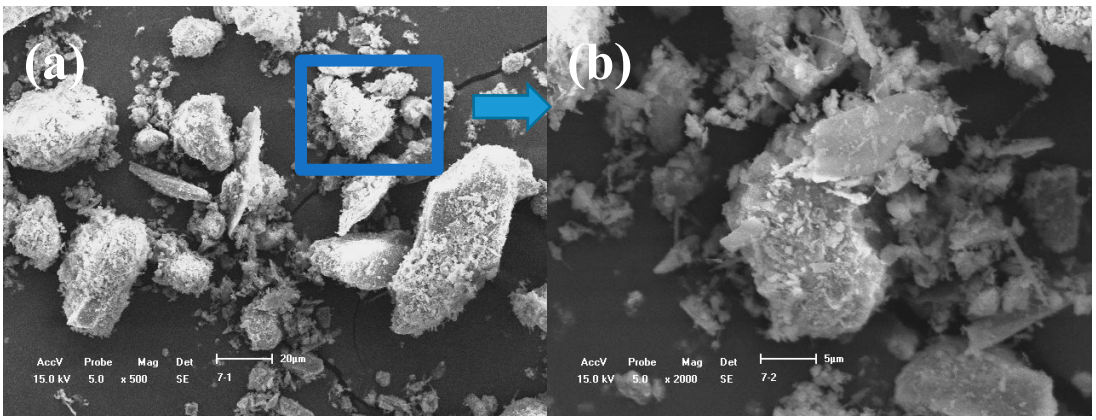

Figure 2. Scanning electron microscope (SEM) pattern of the boron-bearing iron tailings: (**a**)-particle distribution; (**b**)-partial region enlarged.

2.2. Product Analysis

In the final leach liquor, the concentration of Fe was measured by an ultraviolet-visible photometer (Beijing PUXI, SF2-7520, Beijing China). The concentration of Mg was determined while using an EDTA complexation titration method (Mg and Ca complexation method, the error was less than 0.2%). The concentration of Mg was determined while using an EDTA titration method (the error was less than 0.2%). The roasting products and residues were identified using a D/max RB X-ray diffraction instrument (Rigaku Corporation, D/max-RB, Tokyo, Japan) with Cu-Kα radiation ranging from 5~80° and a scanning speed of 10°/min. The analysis of the morphology of the roasted products was conducted while using a Scanning Electron Microscope (Shimadzu, SSX-550, Tokyo, Japan).

Thermogravimetric-differential scanning calorimeter (TG-DSC) analysis of the boron-bearing iron tailings was determined using a differential scanning calorimetry- thermal Gravity (NETZSCH STA449F3A-1001-M, Selb, German) instrument operated in a flowing Ar (purity > 99.999%) atmosphere, with a heating rate of 10 °C/min. from room temperature to 800 °C.

2.3. Methods and Procedures

The boron-bearing iron tailings were grounded into fine powder in ball mill equipment (BS2308, TENCAN POWDER, China). Subsequently, the ore powder and a certain amount of ammonium sulfate

were blended and put it into a ceramic crucible. The crucible was placed in a resistance furnace (DB2, Tianjin Zhonghuan Furnace Corp., Tianjin, China) with an automated temperature control unit and a tail gas instrument. After roasting at the specified temperature for a certain amount of time, the roasted products were cooled to room temperature. Afterwards, the roasted products were ground and leached with deionized water in a constant temperature water bath (DK-524-type, Changzhou Jintan Scientific Instrument Technology, Changzhou, China) at 90 °C for 30 min. The resultant liquor was leached, filtered using a vacuum filtration system, and the remaining solids were then washed twice with deionized water. The filtrate was analyzed to determine the concentration of iron, aluminum, and magnesium leached. Figure 3 shows the schematic diagram of the roasting reaction system.

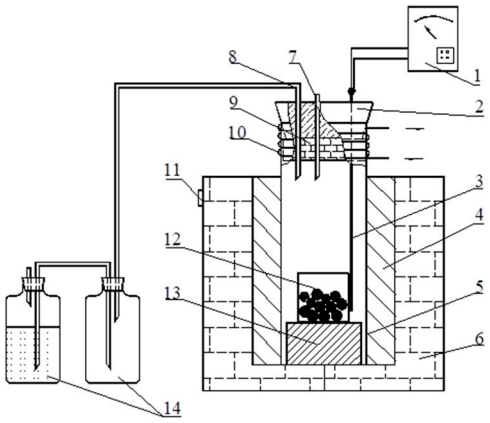

Figure 3. Schematic diagram of the roasting reaction system. 1. intelligent programmable regulator; 2. rubber stopper; 3. thermocouple; 4. Brusque; 5. reaction still; 7. resistance wire heater; 7. gas inlet; 8. gas outlet; 9. refractory bricks; 10. Copper cooling system; 11. binding post; 12. corundum crucible; 13. refractory bricks; 14. gas collecting bottle.

3. Results and Discussion

3.1. Roasting Process

The roasting products were leached at 90 °C for 30 min.

3.1.1. Effect of the Molar Ratio of Ammonium Sulfate to Ore

The effect of the molar ratio of ammonium sulfate to ore on the extractions of magnesium, aluminum, iron, and boron were investigated at the roasting temperature of 450 °C, the roasting time of 120 min., and the ore particles size of less than 80 μm. Figure 4 presents the results.

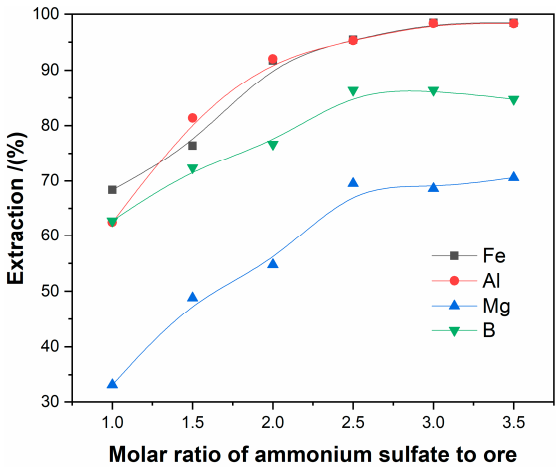

Figure 4. The effect of the molar ratio ammonium sulfate to ore on the extraction of elements.

It is shown in Figure 4 that the extractions rate of iron, aluminum, magnesium, and boron increase with the ammonium-to-ore molar ratio, and reach their maximum at 3:1.

3.1.2. Effect of Roasting Temperature

The influence of the roasting temperature from 250 °C to 500 °C on the extractions of iron, aluminum, magnesium, and boron was studied under the condition of the molar ratio of ammonium sulfate to tailings of 3:1, roasting time of 120 min., and the ore particles size of less than 80 μm.

As seen in Figure 5, there are significant improvements in the extraction of iron, aluminum, and magnesium when the roasting temperature is increased from 250 °C to 450 °C, and the extraction reaches the maximum values for each of the metals at 450 °C. The extraction of boron firstly increases and then decreases with the enhanced roasting temperature, and reaches the maximum at 400 °C. The increase of the extractions of iron, aluminum, and magnesium results from the increasing reaction activity of ammonium sulfate with increased temperature. However, the decrease in the extraction of boron can be attributed to the volatilization of boron oxide at high temperature. Thus, the roasting temperature of 450 °C was applied in the following experiments. The roasting mechanism will be discussed in detail in the following section.

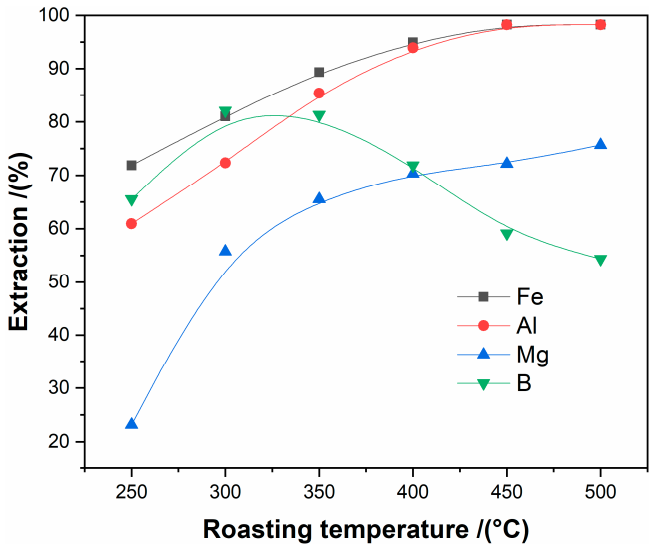

Figure 5. The effect of roasting temperature on the extraction of metals.

3.1.3. Effect of Roasting Time

The effect of roasting time from 20 min. to 160 min. on the extraction of iron, aluminum, and magnesium was studied under the conditions of the molar ratio of ammonium sulfate to tailings of 3:1, the roasting temperature of 450 °C, and the ore particles size of less than 80 μm.

As can be seen from Figure 6, the extraction of iron, aluminum, and magnesium rapidly increased from 20 min. to 120 min. The maximum extraction was reached at 120 min., indicating that the sulfating process of iron, aluminum, and magnesium are close to completion at 120 min. While the extraction of boron firstly increases but then decreases with the prolonging of roasting time, resulting from the increasing of the volatilization of boron oxide. Therefore, the roasting time of 120 min. was applied in subsequent experiments.

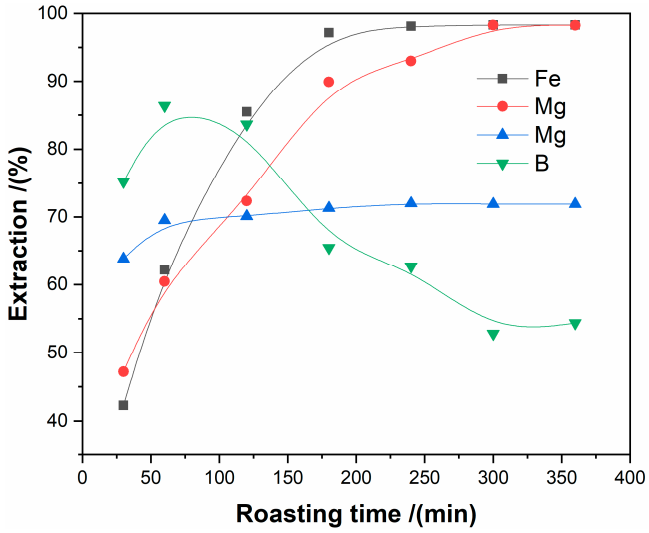

Figure 6. The effect of roasting time on the extraction of metals.

3.1.4. Effect of the Particle Size the Tailings

The effect of the particle size from 40 μm to 120 μm on the extractions of iron, aluminum, magnesium, and boron was studied under the condition of ammonium-to-ore mole ratio of 3:1, roasting temperature of 450 °C, and roasting time of 120 min.

The results (as seen in Figure 7) show that all metal extractions are increasing with declining particle size. All elements extractions reach the maximum at the particle size of less than 80 μm. The extractions were not improved with the reduced size.

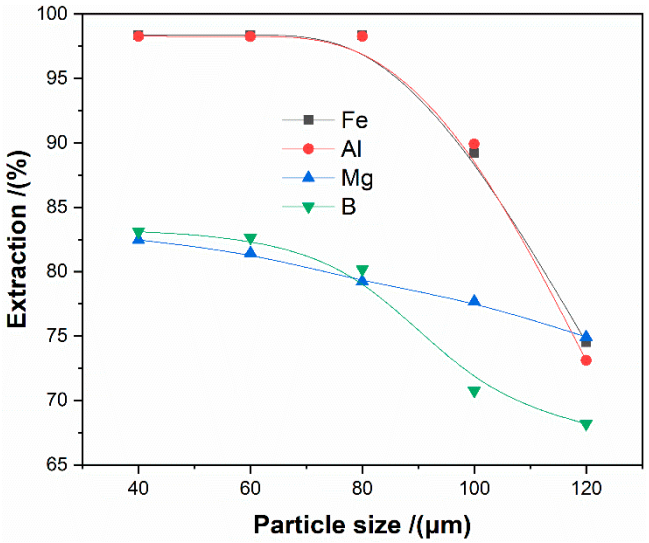

Figure 7. The effect of the particle size on the extraction of metals.

3.1.5. Orthogonal Design of Experiments

An orthogonal experiment of $L_9(3^4)$ was designed based on the single factor experiment in order to obtain the optimal reaction conditions of the roasting process. The factors of roasting temperature (A), the molar ratio of the ammonium sulfate to boron-bearing iron tailings (B), the roasting time (C), and particle size of tailings (D), the selected factors and levels are listed in Table 2. Table 3 shows the orthogonal experimental results.

Table 2. Experimental factors and levels.

Level No.	Factor			
	A/°C	B/h	C/min	D/μm
1	350	2	80	120
2	400	2.5	100	100
3	450	3	120	80

Table 3. Results of $L_9(3^4)$ orthogonal experiments.

No.	Factor							
	A/°C	B/h	C/min	D/μm	Fe	Al	Mg	B
1	350	2	80	120	71.40	72.91	57.72	76.58
2	350	2.5	100	100	74.37	76.31	69.14	80.39
3	350	3	120	80	83.89	85.22	79.89	81.07
4	400	2	100	80	75.27	76.87	71.72	82.47
5	400	2.5	120	120	78.34	78.63	82.47	84.71
6	400	3	80	100	80.02	82.41	81.71	83.01
7	450	2	120	100	80.13	70.73	78.41	70.14
8	450	2.5	80	80	78.01	79.44	84.98	69.58
9	450	3	100	120	82.09	82.68	85.31	68.31
Fe Average1	76.55	75.60	76.81	77.28				
Fe Average2	78.21	76.91	77.24	78.51				
Fe Average3	80.08	82.30	80.79	79.06				
R of Fe extraction	3.53	6.70	3.98	1.78	$R_B>R_C>R_A>R_D$			
Al Average1	78.14	76.83	78.25	78.07				
Al Average2	79.30	78.12	78.62	79.81				
Al Average3	80.95	83.43	81.52	80.51				
R of Al extraction	2.803	6.600	3.274	2.437	$R_B>R_C>R_A>R_D$			
Mg Average1	76.243	75.013	76.287	76.540				
Mg Average2	77.843	76.727	76.513	77.720				
Mg Average3	78.787	81.133	80.073	78.613				
R of Mg extraction	2.544	6.120	3.786	2.073	$R_B>R_C>R_A>R_D$			
B Average1	79.347	76.397	76.390	76.533				
B Average2	83.397	78.277	77.057	77.847				
B Average3	69.343	77.643	78.640	77.707				
R of B extraction	17.054	1.830	2.250	1.314	$R_A>R_C>R_B>R_D$			

As shown in Table 3, the orthogonal experimental results show the effect of the four factors on the extraction of metals, as follows: the molar ratio of ammonium sulfate to tailings, the roasting time, the roasting temperature, and the particle size of the tailings. Figure 8 shows the trend of the range. It can be seen that the optimum conditions of the roasting process are the roasting temperature of 450 °C, the roasting time of 120 min., the molar ratio of ammonium sulfate to tailings of 3:1, and the particle size of the tailings of less than 80 μm. According to the optimized process conditions, the experimental verification shows that the extractions of Fe and Al all exceed 98%, while the extraction of Mg and B all exceed 80%.

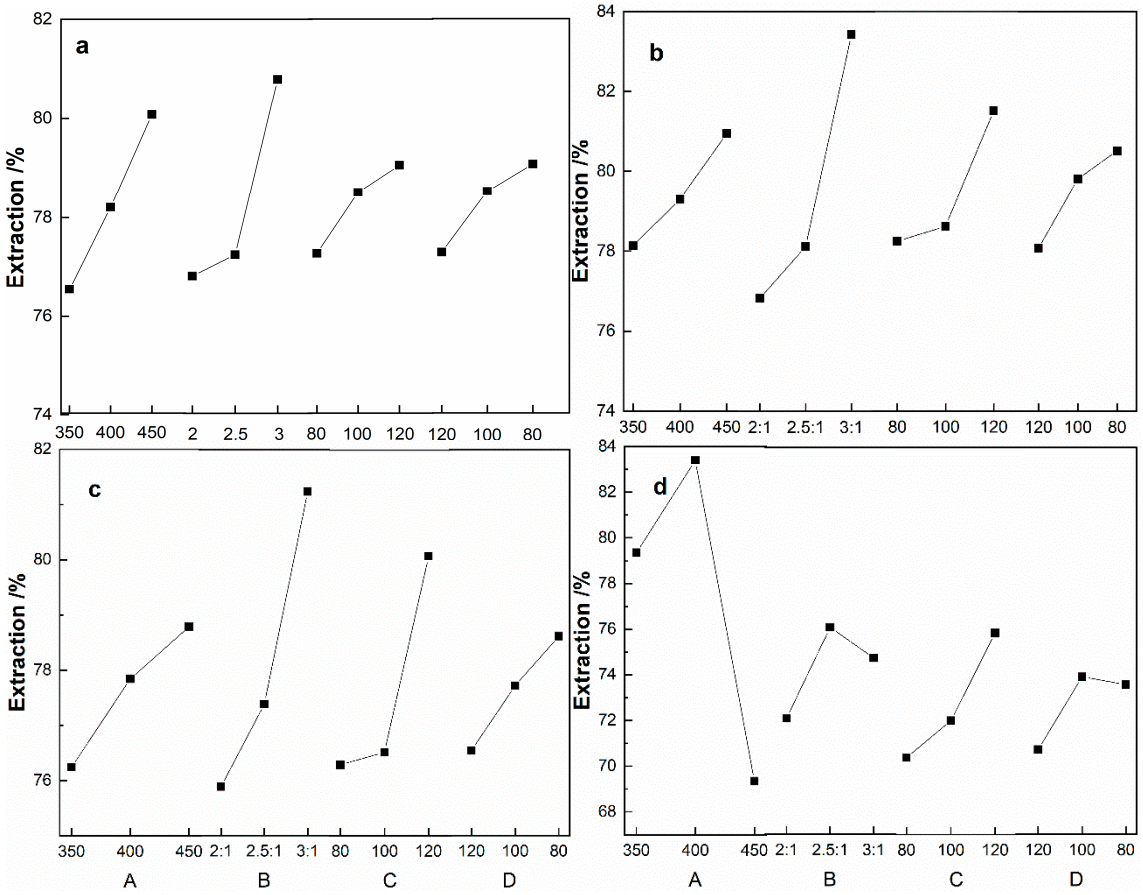

Figure 8. Trend chart of range: a-Fe; b-Al; c-Mg; d-B for the factors of roasting temperature (**a**), the molar ratio of the ammonium sulfate to boron-bearing iron tailings (**b**), the roasting time (**c**) and particle size of tailings (**d**).

3.2. Roasting Mechanism and Kinetics

3.2.1. The Roasting Mechanism

Figure 9 shows the DSC-TG curves of the ammonium sulfate (Figure 9a) and the mixture of ammonium sulfate and tailings with a molar ratio of 1:3 (Figure 9b) from room temperature to 800 °C at a heating rate of 10 °C/min. As seen in Figure 8a, there are two obvious endothermic peaks at approximately 289 °C and 393 °C, which corresponded to the decomposition of $(NH_4)_2SO_4$ (Equation (1)) and the decomposition of NH_4HSO_4 (Equation (2)), respectively, while there are two stages of mass loss corresponding to the two stages decomposition [30]. It can be seen from Figure 9b that there are two endothermic peaks at approximately 318 °C and 439 °C on the DSC curve, corresponding two large weight losses that were observed from the TG curve at two different temperature ranges of 240–359 °C and 359–448 °C. The first endothermic peak can be attributed to the sulfation reactions between $(NH_4)_2SO_4$ and the tailings, while the second endothermic peak can be attributed to the sulfation reactions between NH_4HSO_4 and the tailings, the sulfation reactions are shown in Equations (3)–(8). The followed mass loss on the TG curve can be attributed to the decomposition of ammonium metal sulfates (as shown in Equations (9)–(11)).

Figure 10 shows the XRD patterns of samples that were obtained at different roasting temperatures. It can be seen that the main phases at the roasting temperature of 300 °C are lizardite ($Mg_3Si_2O_5(OH)_4$) phase, ferric sulfate ($Fe_2(SO_4)_3$), ammonium ferric sulfate ($(NH_4)_3Fe(SO_4)_3$), ammonium magnesium sulfate ($(NH_4)_2Mg(SO_4)_2$), and ammonium hydrogen sulfate (NH_4HSO_4), indicating that the decomposition of ammonium sulfate is not complete and that part of the mineral phases have reacted and generated corresponding metal sulfates. The diffraction peaks of szaibelyite ($MgBO_2(OH)$),

magnetite phase (Fe_3O_4), and halloysite phase ($Al_2Si_2O_5(OH)_4(2H_2O)$ appear on the samples that were produced at the roasting temperature of 350 °C. When the roasting temperature is 400 °C, the diffraction peaks of ammonium sulfate disappear and the diffraction peaks of metal sulfate intensify, which indicates that the decomposition of ammonium sulfate is complete and the generation of metal sulfates is increased. Additionally, when the roasting temperature is 450 °C, the diffraction peaks of ammonium sulfate become weak, but the diffraction peaks of ferric sulfate significantly intensify. These results show that parts of the ammonium metal sulfates are decomposed at this temperature. The sulfation roasting process with ammonium sulfate demonstrates that the metal-bearing mineral phases react with ammonium sulfate and ammonium bisulfate to form ammonium metal sulfates. As the roasting temperature increases, ammonium metal sulfates begin to decompose into corresponding metal sulfate. However, the diffraction peaks of boron-bearing phases are not detected.

The total chemical reactions between the minerals of the tailings and ammonium sulfate can be given, as follows.

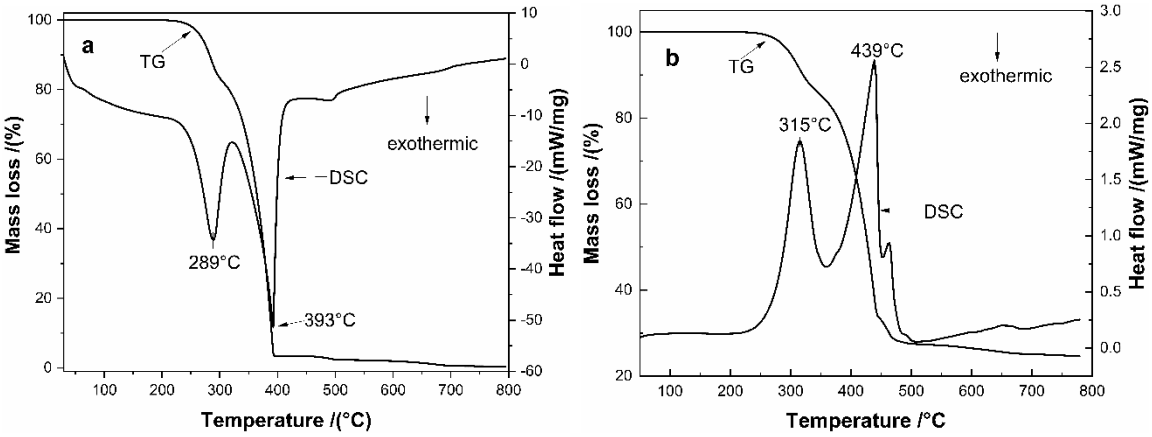

Figure 9. Differential thermal analysis curve of ammonium sulfate and the mixture of and raw tailings and ammonium sulfate: (**a**) ammonium sulfate; and (**b**) the mixture of ammonium sulfate and raw tailings.

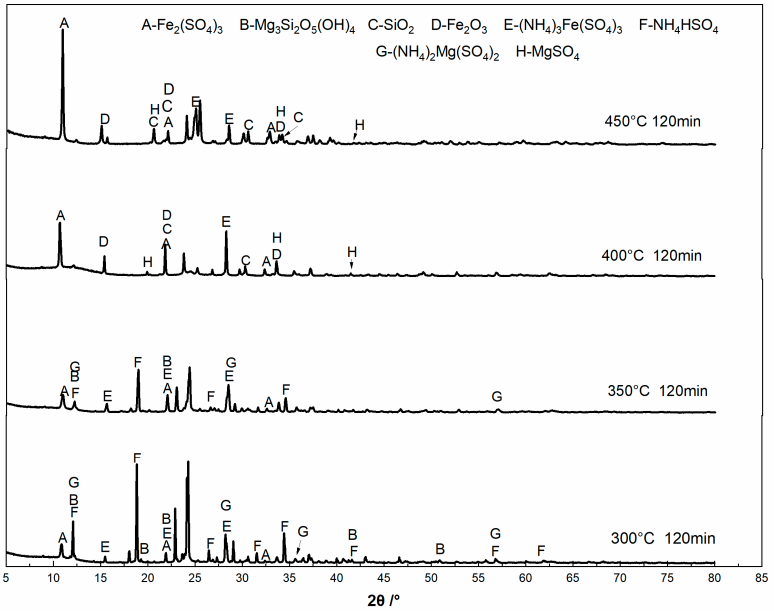

Figure 10. XRD of residue obtained at different roasting temperatures.

$$(NH_4)_2SO_4 \rightarrow NH_4HSO_4 + NH_3(g) \quad (1)$$

$$NH_4HSO_4 \rightarrow NH_3(g) + SO_3(g) + H_2O(g) \quad (2)$$

$$Fe_2O_3 + 4(NH_4)_2HSO_4 \rightarrow 2NH_4Fe(SO_4)_2 + 3H_2O(g) + 6NH_3(g) \quad (3)$$

$$Fe_2O_3 + 4NH_4HSO_4 \rightarrow 2NH_4Fe(SO_4)_2 + 3H_2O(g) + 2NH_3(g) \quad (4)$$

$$Mg_3Si_2O_5(OH)_4 + 6(NH_4)_2SO_4 \rightarrow 3(NH_4)_2Mg(SO_4)_2 + 2SiO_2 + 5H_2O(g) + 6NH_3(g) \quad (5)$$

$$Mg_3Si_2O_5(OH)_4 + 6NH_4HSO_4 \rightarrow 3(NH_4)_2Mg(SO_4)_2 + 2SiO_2 + 5H_2O(g) \quad (6)$$

$$Mg_2(B_2O_5)(H_2O) + (NH_4)_2SO_4 \rightarrow 2(NH_4)_2Mg(SO_4)_2 + B_2O_3 + 4NH_3(g) + 3H_2O(g) \quad (7)$$

$$Mg_2Si_5Al_4O_{18} + 12(NH_4)_2SO_4 \rightarrow 4NH_4Al(SO_4)_2 + 2(NH_4)_2Mg(SO_4)_2 + 5SiO_2 + 4NH_3(g) + 8H_2O(g) \quad (8)$$

$$2NH_4Fe(SO_4)_2 \rightarrow Fe_2(SO_4)_3 + H_2O(g) + 2NH_3(g) + SO_3(g) \quad (9)$$

$$(NH_4)_2Mg(SO_4)_2 \rightarrow MgSO_4 + H_2O(g) + 2NH_3(g) + SO_3(g) \quad (10)$$

$$2NH_4Al(SO_4)_2 \rightarrow Al_2(SO_4)_3 + H_2O(g) + 2NH_3(g) + SO_3(g) \quad (11)$$

Figure 11 gives the SEM images of the samples that were roasted at different temperature under the conditions that the roasting time of 120 min., the molar ratio of ammonium sulfate to tailings of 3:1, and the particle size of the tailings of less than 80 μm; as seen in Figure 10a, the roasted product at 300 °C presents a thick, cubic plate structure, and smooth surface. With roasting temperature continually increasing, the plate is cracked, the size of roasted product shrinks (400 °C, Figure 10c), and the surface of the particle changes from smooth to rough from 300 to 450 °C (Figure 10a–d).

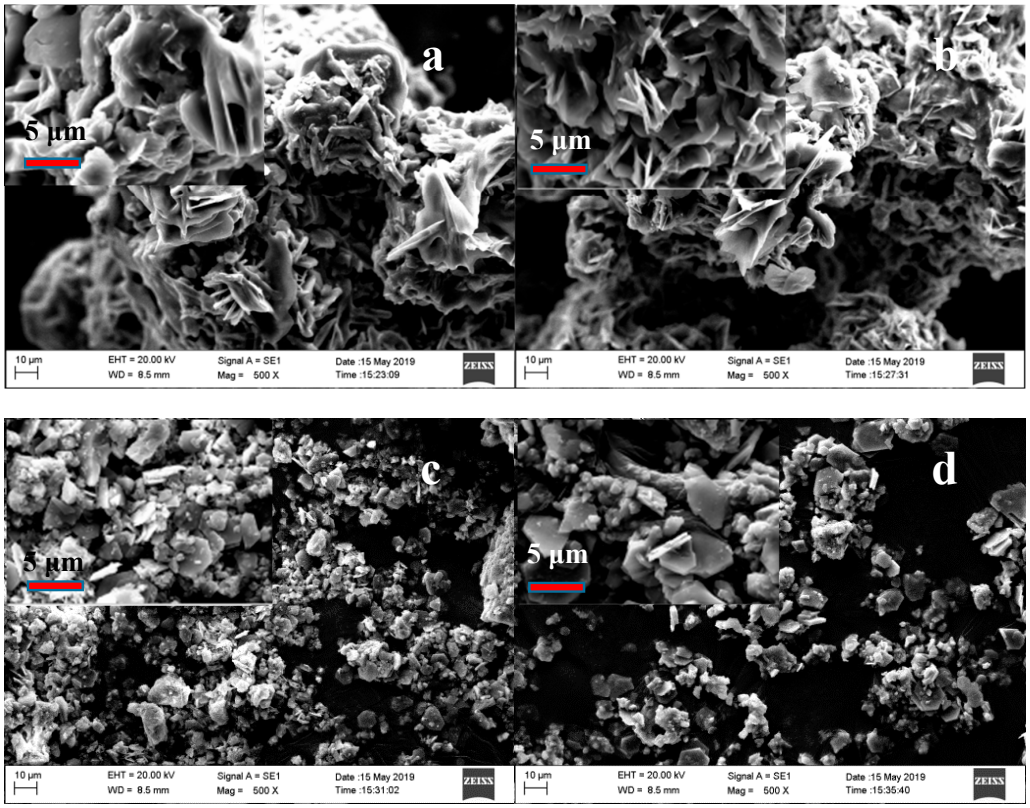

Figure 11. SEM images of residues after roasting at specified temperatures: (**a**). 300 °C; (**b**). 350 °C; (**c**). 400 °C; and, (**d**). 450 °C.

3.2.2. Kinetic Analysis

Figure 12 shows the extractions of Fe, Al, Mg, and B at 250–450 °C varying the different time (molar ratio of ammonium sulfate to ore of 3:1, particle size of less than 80 μm).

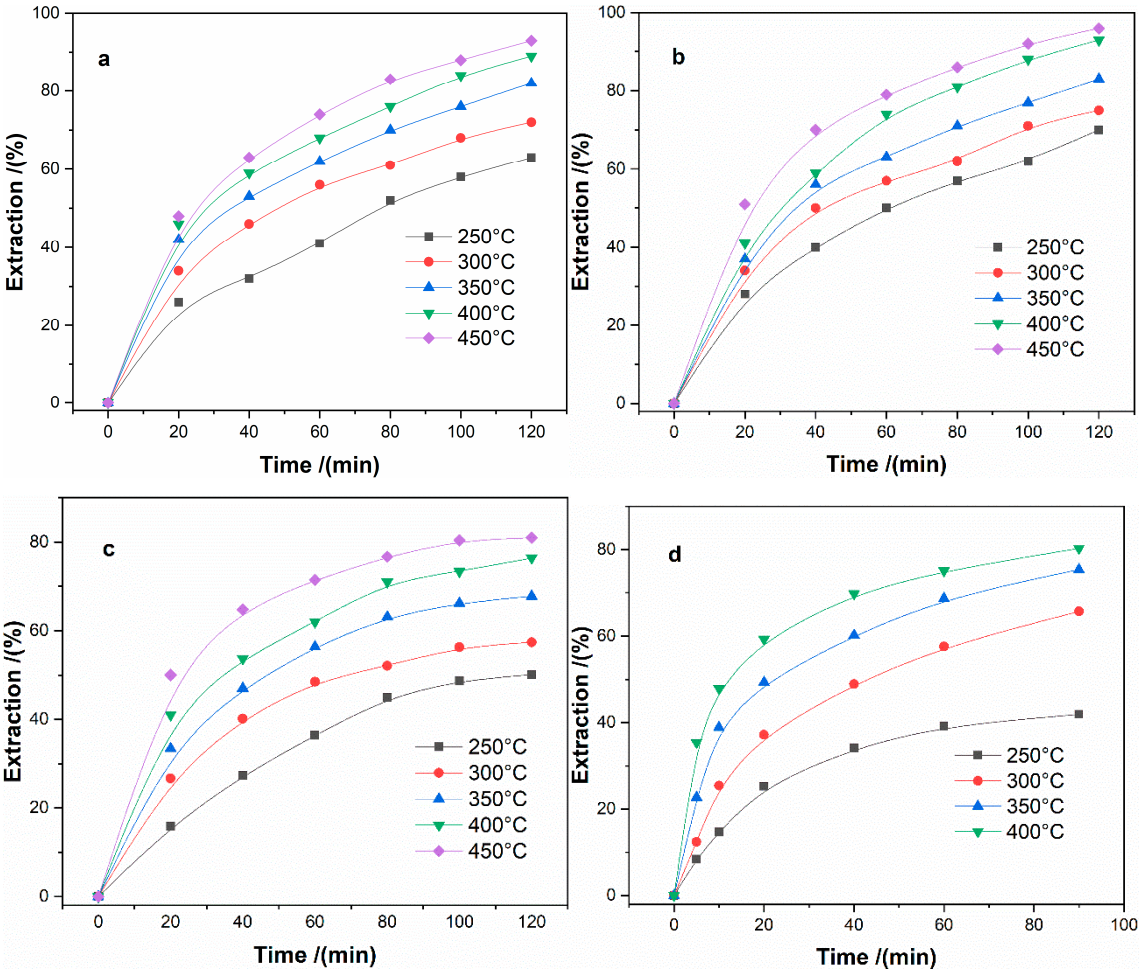

Figure 12. Extraction of metals at different roasting temperatures as a function of roasting time: (**a**)-Fe; (**b**)-Al; (**c**)-Mg; and, (**d**)-B.

The system where sulfation roasting to boron-bearing iron tailings with ammonium sulfate is a liquid-solid reaction, which can be analyzed by the shrinking core model. If the sulfation reactions are controlled by the phase boundary reaction (R_3), the following expression of the model can be used to describe the kinetics of the process:

$$1 - (1 - \alpha)^{1/3} = k_c t \quad (12)$$

However, if the sulfation reactions are controlled by the three-dimensional diffusion (internal diffusion), the G-B equation (D_4) [31] can be described as:

$$1 - 2/3\alpha - (1 - \alpha)^{2/3} = k_p t \quad (13)$$

where α is the extraction ratio of Fe, Al, and Mg, k_c and k_p is the reaction rate constant (min.$^{-1}$), t is reaction time (min.).

The experimental data were used to fit the suitable mechanism function in the sulfation roasting process. The results showed that the fitting results by the G-B equation have more positive correlation coefficients than the phase boundary reaction equation; hence, the G-B equation was applied in the fitting of the experimental data and the results are shown in Figure 13. As seen, $1 - 2/3\alpha - (1 - \alpha)^{2/3}$

has a good linear relationship against the reaction time for Fe, Al, and Mg, which indicates that the sulfation process to boron-bearing iron tailings is controlled by internal diffusion. According to Arrhenius equation $k = Ae^{-E_a/RT}$, $\ln k = \ln A - E_a/RT$, the apparent activation energy can be obtained from the slope of the plot of $\ln k$ vs. 1/T, and the pre-exponential factor can be obtained by intercept, the fitting results of $\ln k$ vs. 1/T are shown in Figure 14. The apparent activation energy of each metal is calculated as 17.10 kJ·mol^{-1}, 17.85 kJ·mol^{-1}, 19.79 kJ·mol^{-1}, and 29.71 kJ·mol^{-1} for Fe, Al, Mg, and B, respectively. Additionally, the pre-exponential factor is calculated as 0.0338, 0.0392, 0.0339, and 0.3265 for Fe, Al, Mg, and B, respectively. Therefore, the equation between the reaction rate (α) and reaction time (t) can be written as Equations (13)–(15) for Fe, Al, and Mg, respectively.

$$1 - 2/3\alpha - (1-\alpha)^{2/3} = 0.0338\exp(-17100/RT)t \quad (14)$$

$$1 - 2/3\alpha - (1-\alpha)^{2/3} = 0.0392\exp(-17850/RT)t \quad (15)$$

$$1 - 2/3\alpha - (1-\alpha)^{2/3} = 0.0339\exp(-19790/RT)t \quad (16)$$

$$1 - 2/3\alpha - (1-\alpha)^{2/3} = 0.3265\exp(-29710/RT)t \quad (17)$$

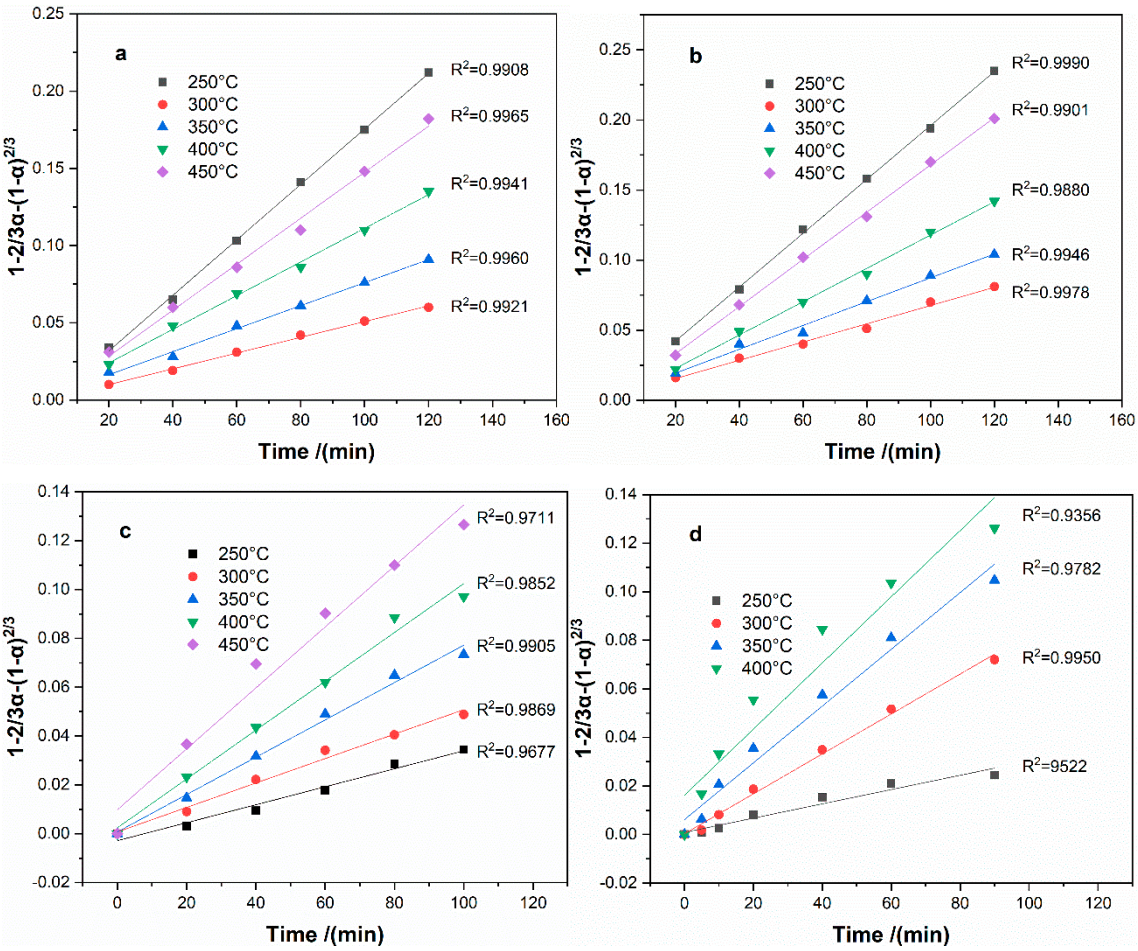

Figure 13. Plots of 1-2/3α-(1-α)$^{2/3}$ vs roasting time at different roasting temperatures: (**a**)-Fe; (**b**)-Al; (**c**)-Mg; and, (**d**)-B.

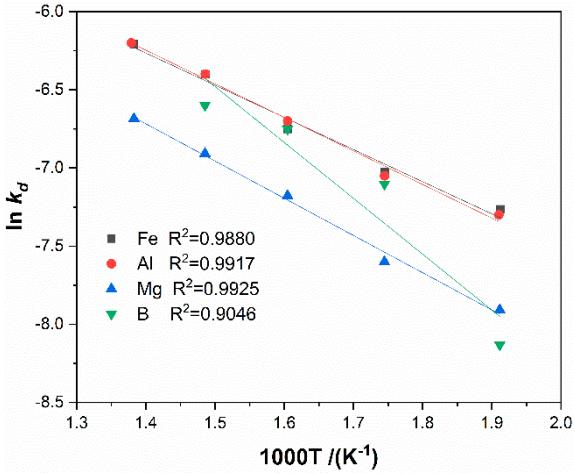

Figure 14. Arrhenius plot for roasting boron-bearing iron tailings with ammonium sulfate.

3.3. Leaching Residue Analysis

The leaching residue was obtained under the conditions that the roasting temperature of 450 °C, the roasting time of 120 min., the molar ratio of ammonium sulfate to tailings of 3:1 and the particle size of the tailings of less than 80 μm, the XRD patterns and the SEM image are shown in Figure 15. As seen, the main phases in the residue are ferric oxide serpentine ($Mg_3SiO_5(OH)_4$) talc ($Mg_3Si_4O_{10}(OH)_2$) and quartz (SiO_2). The leaching residue presents fluffy bulbous that reunite together.

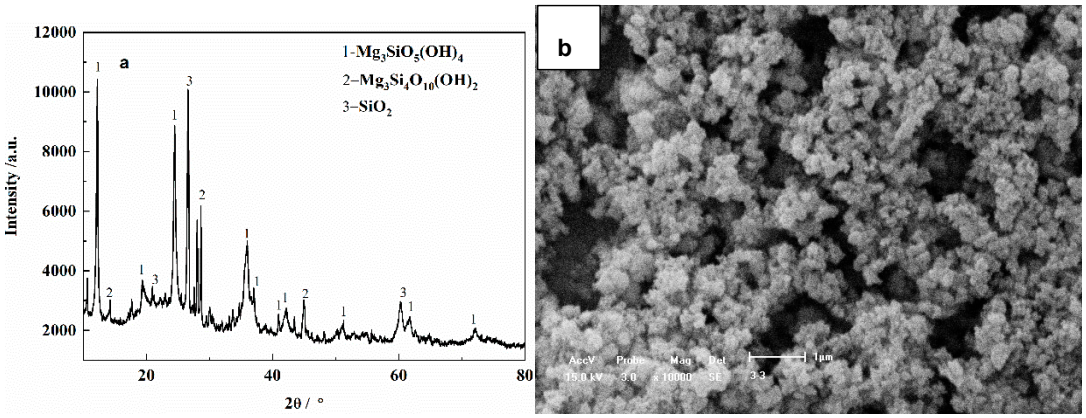

Figure 15. XRD patterns and SEM image of the leaching residue: a-XRD patterns; b-SEM image.

4. Conclusions

In this study, a clean process was proposed to process a large amount of boron bearing iron tailings in China. The results that were obtained in this study are as follows:

(1) The optimal sulfation roasting conditions using ammonium sulfate for boron-bearing iron tailings are that the roasting temperature is 450 °C, the roasting time is 120 min., the molar ratio of ammonium sulfate to tailings is 3:1, and the particle size is less than 80 μm. These conditions yield more than 98% extraction of Fe and Al, and more than 80% extraction of Mg and B. These findings were obtained from both single factor and orthogonal experiments.

(2) The sulfation reactions between ammonium sulfate and the tailings can be divided into two steps, the reactions between ammonium sulfate and the tailings at 240–359 °C, and the reactions between ammonium bisulfate at 359–448 °C. The mineral phase transformation in the roasting process can be described by the sequence of mineral phases→ammonium metal sulfates→metal sulfates.

(3) The kinetics analysis indicates that internal diffusion controls the sulfation reactions of metals. The apparent activation energies of the reactions are 17.10 kJ·mol^{-1}, 17.85 kJ·mol^{-1}, 19.79 kJ·mol^{-1}, and 29.71 kJ·mol^{-1} for Fe, Al, Mg, and B, respectively.

The proposed process can comprehensively utilize the elements in the born-bearing iron tailings at low temperatures and with no additional waste slag being generated, which could be given a guide to process similar waste solid slags.

Author Contributions: X.L. performed the experiment, analysis of the data and contributed to writing the draft paper; F.C. contributed to the aspects related to the processing figures, kinetic analysis, and writing the paper; Z.N. performed the generating the results and microstructural work; M.L.F. performed the language and the quality of the paper; Y.Z. provided the fund and the experimental design.

Funding: This research received no external funding.

Conflicts of Interest: The authors declare no conflict of interest.

References

1. Jiang, S.Y. Boron isotope geochemistry of hydrothermal ore deposits in China: A preliminary study. *Phys. Chem. Earth Part A Sol. Earth Geod.* **2001**, *26*, 851–858. [CrossRef]
2. Kistler, R.B.; Helvaci, C. Boron and borates. *Ind. Miner. Rocks.* **1994**, *6*, 171–186.
3. Kar, Y.; Şen, N.; Demirbaş, A. Boron minerals in Turkey, their application areas and importance for the country's economy. *Miner. Energy Raw Mater. Rep.* **2006**, *20*, 2–10. [CrossRef]
4. Qiao, X.; Li, W.; Zhang, L.; White, N.C.; Zhang, F.; Yao, Z. Chemical and boron isotope compositions of tourmaline in the Hadamiao porphyry gold deposit, Inner Mongolia, China. *Chem. Geol.* **2019**, *519*, 39–55. [CrossRef]
5. Li, G.; Liang, B.; Rao, M.; Zhang, Y.; Jiang, T. An innovative process for extracting boron and simultaneous recovering metallic iron from ludwigite ore. *Miner. Eng.* **2014**, *56*, 57–60. [CrossRef]
6. Ding, Y.G.; Wang, J.S.; Wang, G.; Ma, S.; Xue, Q.G. Comprehensive utilization of paigeite ore using iron nugget making process. *J. Iron Steel Res. Int.* **2012**, *19*, 9–13. [CrossRef]
7. Wang, G.; Ding, Y.G.; Wang, J.S.; She, X.F.; Xue, Q.G. Effect of carbon species on the reduction and melting behavior of boron-bearing iron concentrate/carbon composite pellets. *Int. J. Miner. Metallurg. Mater.* **2013**, *20*, 522–528. [CrossRef]
8. Jie, L.; Fan, Z.G.; Liu, Y.L.; Liu, S.L.; Jiang, T.; Xi, Z.P. Preparation of boric acid from low-grade ascharite and recovery of magnesium sulfate. *Tran. Nonferrous Met. Soc. China* **2010**, *20*, 1161–1165.
9. Sivrikaya, O.; Arol, A.I. Use of boron compounds as binders in iron ore pelletization. *Open Min. Process. J.* **2010**, *3*, 25–35. [CrossRef]
10. Ucbeyiay, H.; Ozkan, A. Two-stage shear flocculation for enrichment of fine boron ore containing colemanite. *Sep. Purif. Technol.* **2014**, *132*, 302–308. [CrossRef]
11. Celik, M.; Yasar, E. Effect of temperature and impurities on electrostatic separation of boron minerals. *Miner. Eng.* **1995**, *8*, 829–833. [CrossRef]
12. Boncukcuoğlu, R.; Kocakerim, M.M.; Kocadağistan, E.; Yilmaz, M.T. Recovery of boron of the sieve reject in the production of borax. *Resour. Conserv. Recycl.* **2003**, *137*, 147–157. [CrossRef]
13. Guliyev, R.; Kuşlu, S.; Çalban, T.; Çolak, S. Leaching kinetics of colemanite in potassium hydrogen sulphate solutions. *J. Ind. Eng. Chem.* **2012**, *18*, 38–44. [CrossRef]
14. Liang, B.; Li, G.; Rao, M.; Peng, Z.; Zhang, Y.; Jiang, T. Water leaching of boron from soda-ash-activated ludwigite ore. *Hydrometallurgy* **2017**, *167*, 101–106. [CrossRef]
15. Erdoğan, Y.; Aksu, M.; Demirbaş, A.; Abalı, Y. Analyses of boronic ores and sludges and solubilities of boron minerals in CO2-saturated water. *Resour. Conserve Recycle* **1998**, *24*, 275–283. [CrossRef]
16. Kavcı, E.; Calban, T.; Colak, S.; Kuşlu, S. Leaching kinetics of ulexite in sodium hydrogen sulphate solutions. *J. Ind. Eng. Chem.* **2014**, *20*, 2625–2631. [CrossRef]
17. Qin, S.; Yin, B.; Zhang, Y.; Zhang, Y. Leaching kinetics of szaibelyite ore in NaOH solution. *Hydrometallurgy* **2015**, *157*, 333–339. [CrossRef]
18. Xu, Y.; Jiang, T.; Zhou, M.; Wen, J.; Chen, W.; Xue, X. Effects of mechanical activation on physicochemical properties and alkaline leaching of boron concentrate. *Hydrometallurgy* **2017**, *173*, 32–42. [CrossRef]

19. Xu, Y.; Jiang, T.; Wen, J.; Gao, H.; Wang, J.; Xue, X. Leaching kinetics of mechanically activated boron concentrate in a NaOH solution. *Hydrometallurgy* **2018**, *179*, 60–72. [CrossRef]
20. Liu, S.; Cui, C.; Zhang, X. Pyrometallurgical separation of boron from iron in ludwigite ore. *ISIJ Int.* **1998**, *38*, 1077–1079. [CrossRef]
21. Wang, G.; Xue, Q.; She, X.; Wang, J. Carbothermal reduction of boron-bearing iron concentrate and melting separation of the reduced pellet. *ISIJ Int.* **2015**, *55*, 751–757. [CrossRef]
22. Zhang, X.; Li, G.; You, J.; Wang, J.; Luo, J.; Duan, J.; Zhang, T.; Peng, Z.; Rao, M.; Jiang, T. Extraction of Boron from Ludwigite Ore: Mechanism of Soda—Ash Roasting of Lizardite and Szaibelyite. *Minerals* **2019**, *9*, 533. [CrossRef]
23. Gao, P.; Li, G.; Gu, X.; Han, Y. Reduction Kinetics and Microscopic Properties Transformation of Boron-Bearing Iron Concentrate—Carbon-Mixed Pellets. *Miner. Process. Extr. Metallurg. Rev.* **2019**, *40*, 1–9. [CrossRef]
24. Liu, Y.; Jiang, T.; Liu, C.; Huang, W.; Wang, J.; Xue, X. Effect of microwave pre-treatment on the magnetic properties of Ludwigite and its implications on magnetic separation. *Metallurg. Res. Technol.* **2019**, *116*, 107. [CrossRef]
25. Xu, Y.; Jiang, T.; Zhou, M.; Gao, H.; Liu, Y.; Xue, X. Surface properties changes during a two-stage mechanical activation and its influences on B2O3 activity of boron concentrate. *Miner. Eng.* **2019**, *131*, 1–7. [CrossRef]
26. Su, Q.; Zheng, S.; Li, H.; Hou, H. Boron resource and prospects of comprehensive utilization of boron mud as a resource in China. *Earth Sci. Front.* **2014**, *21*, 325–330.
27. Kasemann, S.; Erzinger, J.; Franz, G. Boron recycling in the continental crust of the central Andes from the Palaeozoic to Mesozoic, NW Argentina. *Contrib. Mineralog. Petrol.* **2000**, *140*, 328–343. [CrossRef]
28. Lyman, J.W.; Palmer, G.R. *Recycling of Neodymium Iron Boron Magnet Scrap*; US Department of the Interior, Bureau of Mines: Salt Lake City, UT, USA, 1993.
29. Allen, R.P.; Morgan, C.A. Boric Acid Process. U.S. Patent 3,953,580, 27 April 1976.
30. Cui, F.; Mu, W.; Wang, S.; Xin, H.; Xu, Q.; Zhai, Y.; Luo, S. Sodium sulfate activation mechanism on co-sulfating roasting to nickel-copper sulfide concentrate in metal extractions, microtopography and kinetics. *Miner. Eng.* **2018**, *123*, 104–116. [CrossRef]
31. Ginstling, A.M.; Brounshtein, B.I. Concerning the diffusion kinetics of reactions in spherical particles. *J. Appl. Chem. USSR* **1950**, *23*, 1327–1338.